symmetry

MDPI

*Article*

# Dynamical Properties of Baryons

**Egle Tomasi-Gustafsson [1,*], Andrea Bianconi [2,3,*] and Simone Pacetti [4,*]**

[1] CEA, IRFU, Département de Physique Nucléaire, Université Paris-Saclay, CEDEX, 91191 Gif-sur-Yvette, France
[2] Dipartimento di Ingegneria dell'Informazione, Università degli Studi di Brescia, 25121 Brescia, Italy
[3] Gruppo Collegato di Brescia, Istituto Nazionale di Fisica Nucleare, 25133 Brescia, Italy
[4] Dipartimento di Fisica e Geologia, INFN Sezione di Perugia, 06123 Perugia, Italy
* Correspondence: egle.tomasi@cea.fr (E.T.-G.); andrea.bianconi@unibs.it (A.B.); simone.pacetti@unipg.it (S.P.)

**Abstract:** The internal structure of composite particles is conveniently described in terms of form factors (FFs)—these are experimentally accessible in annihilation and scattering of elementary reactions, and are theoretically calculable by all models that describe the properties of particles. FFs depend only on one kinematical variable, $q^2$. This is the four-momentum transferred by the virtual photon that carries the interaction. Important developments in accelerator and detector techniques have brought impressive advances, both by extending the kinematical region and by reaching a higher precision. A critical review on the underlying methods and findings in polarized and unpolarized experiments is presented. The unique role played by polarization in determining the ratio of electric to magnetic form factors in the space-like region, and the extraction of individual form factors in the whole kinematical region, are described. Recent results at electron accelerators and electron–positron colliders confirm the existence of periodical structure in the annihilation cross section. We suggest a global framework which describes the dynamical structure of charge distribution in baryons, in order to build a coherent view of the creation and annihilation of baryonic matter.

**Keywords:** hadron structure; form factors; annihilation and scattering reactions



**Citation:** Tomasi-Gustafsson, E.; Bianconi, A.; Pacetti, S. Dynamical Properties of Baryons. *Symmetry* **2021**, *13*, 1480. https://doi.org/10.3390/sym13081480

Academic Editor: Angel Gómez Nicola

Received: 7 July 2021
Accepted: 5 August 2021
Published: 12 August 2021



## 1. Introduction

Electromagnetic form factors (FFs) are fundamental quantities that describe the internal structure of composite particles. Assuming parity and time invariance, the internal structure of any spin-$S$ particle is characterized by $2S+1$ form factors (FFs). A proton (spin-1/2 baryon) is, therefore, characterized by two FFs: the Pauli and Dirac FFs—$F_1$ and $F_2$—or alternatively, the Sachs FFs—electric, $G_E$, and magnetic, $G_M$. Experimental information on FFs is accessible from the measurement of cross section and polarization observables in elementary reactions involving electrons and baryons.

The underlying assumption is that scattering and annihilation reactions—$e^{\pm}p \to e^{\pm}p$ and $e^+e^- \leftrightarrow \bar{p}p$, respectively—occur through the exchange of a virtual photon with four-momentum $q^2$. Theoretically, FFs can be considered as functions that parameterize the hadron electromagnetic current, which depend on one variable only, $q^2$; thereby, they inherit specific analytical properties. Scattering (annihilation) reactions us allow to scan the space (time-like) region of the transferred four-momentum. The different kinematical regions bring different pieces of information. FFs in the space-like (SL) region, where the transferred momentum square is negative, give a spatial picture of the particle at the scale $x$ defined by $Q^2 = -q^2 > 0$ (through the relation between conjugate variables $\sqrt{Q^2}x = 1$, assuming $\hbar = c = 1$). At small $Q^2$ (corresponding to large distances), the variation of the electric FF in $ep$ elastic scattering has been related to the proton root-mean-square radius.

In the time-like (TL) region, accessed by electron–positron annihilation into a nucleon–antinucleon pair, FFs contain information on the processes of creation of baryonic matter signing the evolution in time of the created charge: the leptons annihilate into a virtual

photon and subsequently matter ad antimatter are formed. In the time-reverse process, the baryon–antibaryon pair annihilates into a virtual photon, originating a lepton–antilepton pair.

As these processes are related by the symmetries of the strong and electromagnetic interactions, efforts have been undertaken to provide a global and coherent description of FFs in the whole kinematical region. Due to unitarity, FFs are real functions in the SL region and complex functions in the TL region. However, at very large momenta, TL FFs are expected to be equal to SL FFs (according to the Phragmèn–Lindelöf theorem), so that they could become real (or differ by a phase of $\pi$).

This paper will focus on proton FFs, where the most recent experimental information is available—for neutrons and other spin-1/2 particles the similar formalisms and considerations apply, however.

## 2. Experimental Determination of Hadron Form Factors

The differential cross section allows, in principle, the determination of the two FFs—electric, $G_E$, and magnetic, $G_M$—that fully characterize the electromagnetic structure of the proton. In the space-like region ($q^2 < 0$), polarization phenomena allow the precise determination of the electric-to-magnetic FF ratio, even at large transferred momenta. The polarization method suggested by A.I. Akhiezer and M.P. Rekalo [1,2] could be applied only recently by the JLab–GEp collaboration [3], due to the availability of high-intensity and high-duty-cycle polarized beams, large angle spectrometers and detectors, and, especially, the development of hadron polarimetry in the GeV region.

In the time-like region, ($q^2 > 0$), the precise measurement of the angular distribution of unpolarized particles allows us, in principle, to determine both of the FFs (in moduli) that contribute with different angular weight. However, due to the luminosity of the electron-positron and proton-antiproton colliders, the statistics collected has not been sufficient until recently, and only a generalized FF corresponding to the hypothesis $G_E = G_M$ could be determined from the integrated cross section.

Interesting results in a large $q^2$ range were obtained by applying the initial state radiation (ISR) method, where a hard photon is emitted with a probability given by a 'radiator function' that depends on its energy and angle. The initial lepton, after emission, is 'quasi-real'. The total cross section can be factorized, disentangling the reaction of interest $e^+e^- \to \bar{p}p$. The benefit of the ISR method is that, by tuning the hard photon kinematics, one can scan a large $q^2$ region with a fixed energy collider. The counterpart, i.e., the loss of cross section by a factor of $\alpha$ ( $\alpha = 1/137$ is the fine electromagnetic constant) due to the emission of an additional photon, is more than compensated by the high luminosity reached in the colliders. At BaBar and BES, this method gave impressive results on the effective FF as well as on the ratio of FFs. However, the individual determination of FFs was only recently obtained at BESIII using the beam scan method.

## 3. Results

### *3.1. Recent Highlights on Space-Like Proton Form Factors*

Assuming single-photon exchange in electron–proton elastic scattering, one can define a *reduced* cross section, $\sigma_{\rm red}$:

$$\begin{aligned} \sigma_{\rm red}(\theta_e, Q^2) &= \left[1 + 2\frac{E}{M}\sin^2(\theta_e/2)\right]\frac{4E^2\sin^4(\theta_e/2)}{\alpha^2\cos^2(\theta_e/2)} \times \epsilon(1+\tau)\frac{d\sigma}{d\Omega} \\ &= \epsilon\, G_E^2 + \tau\, G_M^2\,, \end{aligned} \tag{1}$$

which is linear in the variable $\epsilon = [1 + 2(1+\tau)\tan^2(\theta_e/2)]^{-1}$, where $\theta_e$ is the electron scattering angle in the laboratory frame. The variable $\tau = Q^2/(4M^2)$ is proportional to $Q^2$, $M$ is the proton mass, $E$ is the electron initial energy, and $d\sigma/d\Omega$ is the differential cross section. The Rosenbluth method [4] exploits the linearity of $\sigma_{\rm red}(\epsilon, Q^2)$ at fixed $Q^2$ to determine the FFs squared, $G_E^2$ and $G_M^2$, as the slope and the intercept (multiplied by $\tau$), respectively, of this linear distribution.

Due to the $\tau$ coefficient and to the normalizations $G_E(Q^2 = 0) = 1$ (in units of electric charge) and $G_M(Q^2 = 0) = \mu_p$ ($\mu_p$ is the proton anomalous magnetic moment), increasing $Q^2$ causes the magnetic contribution of the cross section to become larger and larger. For $Q^2 \geq 3\,\mathrm{GeV}^2$, the electric contribution is of the same order or smaller than the experimental error on the cross section, making the potential extraction of $G_E$ doubtful [5].

On the other hand, a measurement of the ratio of transverse ($P_t$) to longitudinal ($P_\ell$) polarization of the recoil proton in the polarized elastic scattering (with linearly polarized electrons) gives a direct measurement of the ratio of electric and magnetic FFs, $R = G_E/G_M$, as found by A.I. Akhiezer and M.P. Rekalo [1,2]:

$$\frac{P_t}{P_\ell} = -2\cot(\theta_e/2)\frac{M}{E+E'}\frac{G_E}{G_M}, \tag{2}$$

($E'$ is the scattered electron energy). Polarization observables, being associated with an interference of amplitudes, are more sensitive to a small contribution of $G_E$ with respect to the differential cross section. From an experimental point of view, one expects smaller errors, as this ratio is free from the systematic errors that come from the beam polarization and the analyzing powers of the polarimeter that cancel in the ratio. The experiments, mostly from the JLab–GEp collaboration [3] and references therein, not only gave more precise results, but also showed that the charge and magnetic distributions in the proton are different from each other, contrary to former belief. It was previously assumed that the proton electric and magnetic form factors have a dipole $\simeq(Q^2)^{-2}$ dependence, which was consistent, on one side, with quark counting rules from QCD [6,7], and on the other side, in a semiclassical approach, with an exponential density distribution. Moreover, the sharp decrease in the FF ratio as a function of $Q^2$, which can be attributed to $G_E$, can be extrapolated to a vanishing, or even negative, electric FF; this is a difficult result to understand.

Future experiments, planned at the 12 GeV JLab accelerator, will bring clarity on this point. The available data, as well as the projection from the future JLab experiment E12-07-109 [8], are shown in Figure 1.

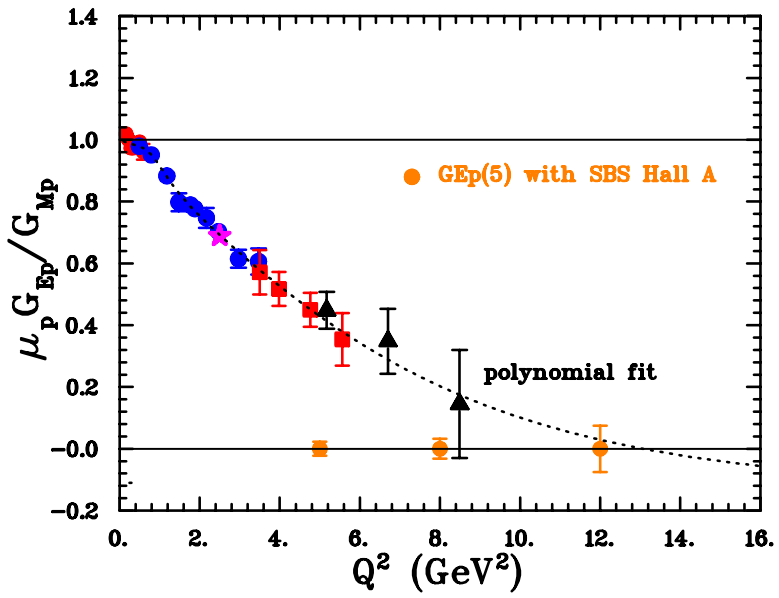


**Figure 1.** Projections of experimental uncertainties for future JLab experiment E12-07-109 [8] (filled orange circles). Previous JLab $G_E^p/G_M^p$ are also shown for comparison [3] and references therein. The dotted line is a polynomial fit.

Note that polarization experiments are made possible by the tremendous progress in hadron polarimetry at the Saturne synchrotron [9,10]. Higher momenta are presently

achievable only in Dubna, where the ALPOM collaboration currently pursues systematic studies [11,12].

### *3.2. The Time-Like Region*

Assuming one-photon exchange and the Born approximation, the differential cross section for the annihilation process $e^+e^- \to \bar{p}p$ in the center of mass system (CMS) is [13]

$$\frac{d\sigma_{e^+e^-\to\bar{p}p}}{d\Omega}(q^2,\theta) = \frac{\alpha^2\beta\,\mathcal{C}(\beta)}{4q^2}\left[\Big(1+\cos^2(\theta)\Big)|G_M|^2 + \frac{1}{\tau}\sin^2(\theta)|G_E|^2\right], \tag{3}$$

where $\beta = \sqrt{1-1/\tau}$ is the velocity of the final hadron and $\theta$ is the antiproton emission angle. The function $\mathcal{C}(\beta)$ is the Coulomb correction for the $\bar{p}p$ final state interaction [14]. This factor becomes negligible a few MeV above threshold, but it is divergent for $\beta \to 0$. However it is compensated by the phase-space factor $\beta$, and the cross section at threshold is then finite and different from zero.

In the annihilation channel, CMS is preferable: the constraint on the vanishing total momentum in the initial and final channels strongly simplifies the formalism. The angular dependence of the cross section, Equation (3), is a direct consequence of the one-photon exchange mechanism, with a single spin-one photon and assuming parity invariance. The specific $\cot^2\frac{\theta_e}{2}$-dependence of the scattering cross section (1) is directly related to the $\cos^2\theta$ annihilation cross section [15] :

$$\cos^2\theta = \frac{\cot^2\theta_e/2}{1+\tau} + 1. \tag{4}$$

The differential cross section (3) contains the squared moduli of the two FFs, whereas polarization observables allow us to access their relative phase. The knowledge of the differential cross section at a fixed value of the total energy $s = q^2$, and for two different angles $\theta$, allows the separation of $|G_M|^2$ and $|G_E|^2$. This is equivalent to the Rosenbluth separation for elastic $ep$-scattering. In the TL region, at a fixed energy of the collider and with a $4\pi$ detector, this procedure is simpler, as the $\cos\theta$ dependence is measured at once. However, in SL region it is necessary to change two of the kinematical variables–the energy of the initial electron and the electron scattering angle–to acquire several $\epsilon$ points at a fixed momentum transfer. In the TL region, due to a limited number of statistics, the determination of the separated electric and magnetic contributions could not be determined for long time. Few data on the FF ratio were produced by the BaBar [16] and PS170 collaborations [17]. Only very recently could the BESIII collaboration extract $|G_E|$ and $|G_M|$ separately and with a meaningful error in the near-threshold region [18].

From the integrated cross section:

$$\sigma_{e^+e^-\to\bar{p}p} = \frac{4\pi\alpha^2\beta\,\mathcal{C}(\beta)}{3q^2}\left(|G_M|^2 + \frac{1}{2\tau}|G_E|^2\right), \tag{5}$$

one can define a combination of the squared moduli of the FFs, called the effective FF, $F_p(q^2)$ :

$$F_p^2 = \frac{2\tau|G_M(s)|^2 + |G_E(s)|^2}{2\tau+1}. \tag{6}$$

It is equivalent to the assumption that $|G_E| = |G_M|$, which only holds at the reaction threshold.

World data of the effective FF are shown in Figure 2. The recent data from BES, using the ISR method [19] (blue squares) and the beam scan method [18] (green triangles) confirm the regular structures previously found in [20] on the BaBar data [16,21] (black circles). The data can be fitted by damped oscillations overimposed on a monotone decreasing background [22]. The best fit is obtained with a background that is a factor of $q^2$ steeper than the dipole behavior predicted by QCD sum rules.

The blue dash-dotted line corresponds to a constant cross section $\sigma = 0.87$ nb, fitted in the range $0.1 < \sqrt{q^2} < 0.9$ GeV. This is consistent with a point-like proton, suggesting that the proton behaves as a particle without structure in the region just above threshold.

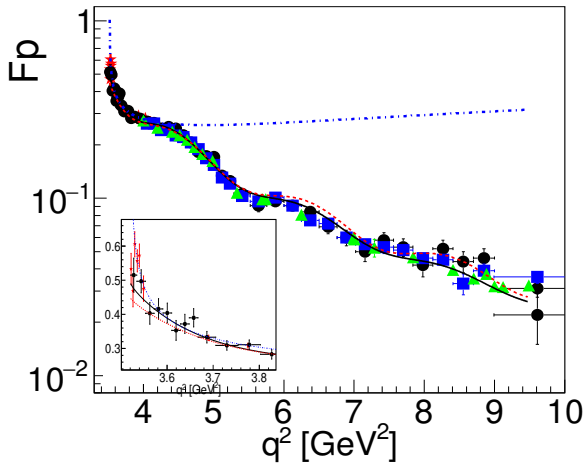


**Figure 2.** Generalized FF as a function of the four-momentum $q^2$. The data are from CMD-3 [23] (red stars), BaBar [16,21] (black circles), BESIII [19] (blue squares), and [18] (green triangles). They are shown together with the six-parameter fit from [22] compared to the fit from [20] (red dashed line). The blue dash-dotted line corresponds to a constant cross section $\sigma = 0.87$ nb.

A recent experiment in the time-like region from the BESIII collaboration [18] at the $e^+e^-$ collider BEPCII, determined for the first time in the TL region the moduli of the electric and magnetic FFs. At the kinematical threshold they should coincide; the precise determination of their value provides a strong constraint for models.

While the SL data (red squares in Figure 3) show a monotone decrease, the TL ones (green triangles in Figure 3) [18], show the presence of oscillations, which do not contradict the results from BaBar [21] (black circles in Figure 3), with a minimum at $q^2 = (5-6)$ GeV$^2$.

In the SL region, the ratio of the moduli of the electric to magnetic FF is expected to have the value $1/\mu_p$ at $q^2 = 0$ (from the FF normalizations) while in the TL region it is constrained by unity at the reaction threshold $q^2 = 4M^2$.

Note that the QCD quark counting rules [6,7] also predict such values at large transferred momenta. The decrease in the ratio in both regions is an indication that the perturbative domain has not yet been reached, and it corroborates the predictions from [24]. Following a similar approach to that for the effective FF, the ratio in the TL region is fitted with a function $F_R$ which reproduces a monopole decrease and a damped oscillation:

$$\begin{aligned} F_R(\omega(s)) &= \frac{1}{1+\omega^2/r_0}\left[1 + r_1 e^{-r_2\omega}\sin(r_3\omega)\right],\ \omega = \sqrt{q^2} - 2m_p\,, \\ r_0 &= (3 \pm 2)\ \text{GeV}^2,\ r_1 = 0.5 \pm 0.1, \\ r_2 &= (1.5 \pm 1.2)\ \text{GeV}^{-1},\ r_3 = (9.3 \pm 0.5)\ \text{GeV}^{-1}, \end{aligned} \tag{7}$$

where the normalization at the production threshold, $F_R(4m_p^2) = 1$, is imposed. The curve representing the fit function, Equation (7), is shown in Figure 3 (black line). The monopole and the oscillatory components are also shown. The TL data on the ratio $R$ are also shown (black circles and green triangles).

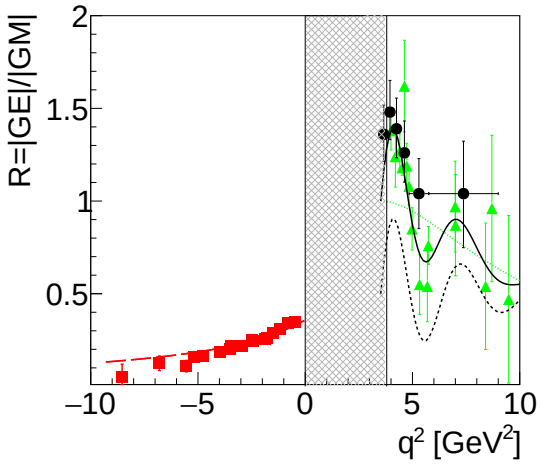


**Figure 3.** Ratio $R = |G_E|/|G_M|$ as a function of $|q^2|$. Symbols as in Figure 2. The fit from Equation (7) (solid black line) is decomposed into the monopole component (green dashed line) and the oscillatory component (black dotted line—shifted up by 0.5). The SL ratio from the JLab–GEp Collaboration [3] is also shown (red squares), fitted by a constrained monopole fit (red long-dashed line).

The red long-dashed line in Figure 3 is a one-parameter monopole function, constrained to $1/\mu_p$ at $q^2 = 0$.

$$f^{SL} = \frac{1}{\mu_p} \frac{1}{\left(1 + \frac{q^2}{a}\right)}; a = 5.4 \pm 0.1 \text{ GeV}^2 \tag{8}$$

Combining the fits of the ratio and of the generalized FF, one can reproduce the moduli of the individual FFs. This is shown in Figure 4 where the extrapolation of the fitting function allows us to determine the expectation at the reaction threshold value: $|G_E(thr)| = |G_M(thr)| = |F_p(thr)| \simeq 0.48$. This number can be compared to the QCD prediction of $F_{\text{th}} \simeq 0.34$ and to the prediction from the VMD model from [25] that gives $F_{\text{th}} \simeq 0.29$, both fitted on the data. The errors on the parameters from the fits are generally of the order of few percent. We can therefore estimate a 5% error to be attributed to the threshold values given above. Note that the VMD model contains five parameters that have physical meaning (masses, couplings, etc.). A new fit, which includes the new data, is highly desirable.

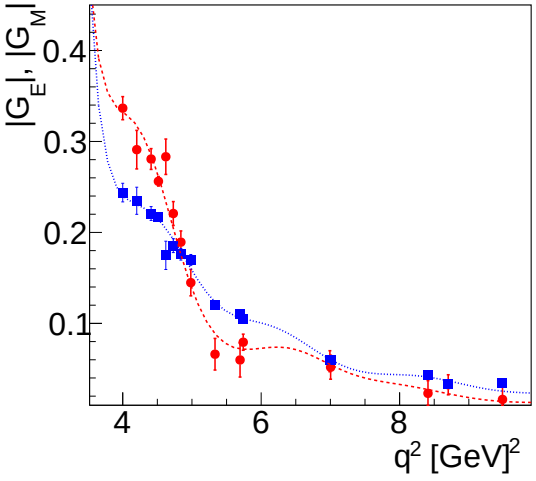


**Figure 4.** $|G_E|$ (red circles) and $|G_M|$ (blue squares) from BESIII. The dashed red (dash-dotted blue) line is the calculation of $|G_E|$ and $|G_M|$ from the fits of the effective FF $F_p$ and the ratio $R$.

## 4. Discussion

In [24], it was suggested that the picture of the nucleon as formed by three constituent quarks does not hold in the center of the nucleon, where a very strong chromomagnetic field produces a screening effect, as in a plasma (short distances corresponding to large transferred momenta). An inner volume inside the nucleon that is electrically neutral induces a faster decrease of the electric FF compared to the magnetic FF in the SL, as well as in the TL region. The magnetic FF follows a $q^2$-dipole behavior and the electric FF an additional $q^2$ decrease, so that the ratio has a monopole $q^2$ dependence.

The regular oscillations have been attributed, in [20], to an interference between two configurations in the formation baryonic matter: one process that occurs at the hadronic scale (about 1 fm) and one at the quark level (0.2 fm). This corroborates the interpretation of TL form factors as describing the time evolution of the electric and magnetic charge from the annihilation point, where a quantum vacuum is created by the energy of the vanishing incident leptons.

In such a frame, one can generalize the definition of FFs, by interpreting the SL and TL FFs, respectively, as projections onto the space (in the Breit frame) and time (in CMS) components of a generalized FF, depending on a space-time variable.

The data on the FF ratio, which is is well-determined up to $|q^2| \simeq 9$ GeV$^2$, point to a very different behavior (in absolute value as well as in shape) in the SL and TL regions. The oscillating behavior seen in the ratio is more evident in the electric than in the magnetic FF.

A measurement of the relative phase, accessible through a single spin polarization observable, would allow us to precisely determine the role and the weight of the two FFs.

Most of the theoretical models have been developed for the SL region, and, when possible, have been analytically continued into the TL region. Some of them are based on parameterizations, with their parameters fixed by the data. As an example, VDM models predict a steeper behavior for $|G_M|$ compared to $|G_E|$, [25]. A number of resonances, in correspondence with light vector mesons, would occur in the unphysical region, i.e., the TL region lying below the production threshold. Note that this region will be accessible through the reaction $\bar{p}p \to e^+e^-\pi^0$ [26,27] at the PANDA@FAIR facility [28] in near future.

The new data that we have discussed call for a revision of the models, aimed at a global understanding of the whole kinematical region, and toward a microscopic description of both annihilation and scattering processes.

**Author Contributions:** Conceptualization, E.T.-G. methodology, S.P.; software, A.B.; validation, E.T.-G., S.P. and A.B.; formal analysis, A.B.; investigation, S.P.; data curation, E.T.-G.; writing—original draft preparation, E.T.-G.; writing—review and editing, A.B., S.P. and E.T.-G. All authors have read and agreed to the published version of the manuscript.

**Funding:** This research received no external funding.

**Institutional Review Board Statement:** Not applicable.

**Informed Consent Statement:** Not applicable.

**Data Availability Statement:** The original data are made publically available by the refererred collaborations. Specific analysis and parameters are available from the authors.

**Conflicts of Interest:** The authors declare no conflict of interest.

## References

1. Akhiezer, A.; Rekalo, M. Polarization phenomena in electron scattering by protons in the high energy region. *Sov. Phys. Dokl.* **1968**, *13*, 572.
2. Akhiezer, A.; Rekalo, M. Polarization effects in the scattering of leptons by hadrons. *Sov. J. Part. Nucl.* **1974**, *4*, 277.
3. Puckett, A.J.; Brash, E.J.; Jones, M.K.; Luo, W.; Meziane, M.; Pentchev, L.; Perdrisat, C.F.; Punjabi, V.; Wesselmann, F.R.; Afanasev, A.; et al. Polarization Transfer Observables in Elastic Electron Proton Scattering at $Q^2$ =2.5, 5.2, 6.8, and 8.5 GeV$^2$. *Phys. Rev. C* **2017**, *96*, 055203; Erratum in *Phys. Rev. C* **2018**, *98*, 019907. [CrossRef]
4. Rosenbluth, M. High Energy Elastic Scattering of Electrons on Protons. *Phys. Rev.* **1950**, *79*, 615–619. [CrossRef]

5. Tomasi-Gustafsson, E. On radiative corrections for unpolarized electron proton elastic scattering. *Phys. Part. Nucl. Lett.* **2007**, *4*, 281–288. [CrossRef]
6. Matveev, V.; Muradyan, R.; Tavkhelidze, A. Automodelity in strong interactions. *Teor. Mat. Fiz.* **1973**, *15*, 332–339. [CrossRef]
7. Brodsky, S.J.; Farrar, G.R. Scaling Laws at Large Transverse Momentum. *Phys. Rev. Lett.* **1973**, *31*, 1153–1156. [CrossRef]
8. Brash, E.; Cisbani, E.; Jones, M.; Khandaker, M.; Liyanage, N.; Pentchev, L.; Perdrisat, C.; Punjabi, V.; Wojtsekhowski, B. Large Acceptance Proton Form Factor Ratio Measurements up to 14.5 GeV$^2$ Using Recoil-Polarization Method. In *JLab Proposal, Experiment E12-07-109*. 2009. Available online: https://www.researchgate.net/profile/Mark-Jones-33/publication/265481523_Update_on_E12-07-109_Large_Acceptance_Proton_Form_Factor_Ratio_Measurements_up_to_145_GeV_2_Using_Recoil-Polarization_Method/links/54f9c0ab0cf25371374ff838/Update-on-E12-07-109-Large-Acceptance-Proton-Form-Factor-Ratio-Measurements-up-to-145-GeV-2-Using-Recoil-Polarization-Method.pdf (accessed on 5 August 2021).
9. Bonin, B.; Boudard, A.; Fanet, H.; Fergerson, R.W.; Garçon, M.; Giorgetti, C.; Habault, J.; Le Meur, J.; Lombard, R.M.; Lugol, J.C.; et al. Measurement of the inclusive $pC$ Analyzing Power and Cross-section in the 1 GeV Region and Calibration of the New Polarimeter POMME. *Nucl. Instrum. Meth. A* **1990**, *288*, 379. [CrossRef]
10. Cheung, N.E.; Perdrisat, C.F.; Oh, J.; Beard, K.; Punjabi, V.; Yonnet, J.; Beurtey, R.; Boivin, M.; Plouin, F.; Tomasi-Gustafsson, E.; et al. Calibration of the polarimeter POMME at proton energies between 1.05-GeV and 2.4-GeV. *Nucl. Instrum. Meth. A* **1995**, *363*, 561–567. [CrossRef]
11. Azhgirey, L.S.; Arefiev, V.A.; Atanasov, I.; Basilev, S.N.; Bushuev, Y.P.; Glagolev, V.V.; Jones, M.K.; Kirillov, D.A.; Korovin, P.P.; Kumbartzki, G.J.; et al. Measurement of analyzing powers for the reaction $\vec{p} + CH_2$ at $p_p$ = 1.75-GeV/c - 5.3-GeV/c. *Nucl. Instrum. Meth. A* **2005**, *538*, 431–441. [CrossRef]
12. Basilev, S.N.; Bushuev, Y.P.; Gavrishchuk, O.P.; Glagolev, V.V.; Kirillov, D.A.; Kostayeva, N.V.; Kovalenko, A.D.; Legostaeva, K.S.; Livanov, A.N.; Philippov, I.A.; et al. Measurement of neutron and proton analyzing powers on $C$, $CH$, $CH_2$ and $Cu$ targets in the momentum region 3–4.2 GeV/c. *Eur. Phys. J. A* **2020**, *56*, 26. [CrossRef]
13. Zichichi, A.; Berman, S.; Cabibbo, N.; Gatto, R. Proton anti-proton annihilation into electrons, muons and vector bosons. *Nuovo Cim.* **1962**, *24*, 170–180. [CrossRef]
14. Hoang, A.H. Two loop corrections to fermion pair production vertices. Electroweak interactions and unified theories. In Proceedings of the 31st Rencontres de Moriond, Leptonic Session, Les Arcs, France, 16–23 March 1996; pp. 129–134.
15. Rekalo, M.P.; Tomasi-Gustafsson, E.; Prout, D. Search for evidence of two photon exchange in new experimental high momentum transfer data on electron deuteron elastic scattering. *Phys. Rev. C* **1999**, *60*, 042202. [CrossRef]
16. Ablikim, M.; Achasov, M.N.; Adlarson, P.; Ahmed, S.; Albrecht, M.; Aliberti, R.; Amoroso, A.; An, Q.; Bai, X.H.; Bai, Y.; et al. Measurement of the $e^+e^- \to p\bar{p}$ cross section in the energy range from 3.0 to 6.5 GeV. *Phys. Rev. D* **2013**, *88*, 072009. [CrossRef]
17. Bardin, G.; Burgun, G.; Calabrese, R.; Capon, G.; Carlin, R.; Dalpiaz, P.; Dalpiaz, P.F.; Derre, J.; Dosselli, U.; Duclos, J.; et al. Determination of the electric and magnetic form-factors of the proton in the timelike region. *Nucl. Phys.* **1994**, *B411*, 3–32. [CrossRef]
18. Ablikim, M.; Achasov, M.N.; Adlarson, P.; Ahmed, S.; Albrecht, M.; Alekseev, M.; Amoroso, A.; An, F.F.; An, Q.; Bai, Y.; et al. Measurement of proton electromagnetic form factors in $e^+e^- \to p\bar{p}$ in the energy region 2.00–3.08 GeV. *Phys. Rev. Lett.* **2020**, *124*, 042001. [CrossRef]
19. Ablikim, M.; Achasov, M.N.; Adlarson, P.; Ahmed, S.; Albrecht, M.; Alekseev, M.; Amoroso, A.; An, F.F.; An, Q.; Bai, Y.; et al. Study of the process $e^+e^- \to p\bar{p}$ via initial state radiation at BESIII. *Phys. Rev. D* **2019**, *99*, 092002, [CrossRef]
20. Bianconi, A.; Tomasi-Gustafsson, E. Periodic interference structures in the timelike proton form factor. *Phys. Rev. Lett.* **2015**, *114*, 232301. [CrossRef]
21. Lees, J.P.; Poireau, V.; Tisser, V.; Grauges, E.; Palano, A.; Eigen, G.; Stugu, B.; Brown, D.N.; Kerth, L.T.; Kolomensky, Y.G.; et al. Study of $e^+ + e^- \to p + \bar{p}$ via initial-state radiation at BABAR. *Phys. Rev. D* **2013**, *87*, 092005. [CrossRef]
22. Tomasi-Gustafsson, E.; Bianconi, A.; Pacetti, S. New fit of timelike proton electromagnetic form factors from $e^+e^-$ colliders. *Phys. Rev. C* **2021**, *103*, 035203. [CrossRef]
23. Akhmetshin, R.R.; Amirkhanov, A.N.; Anisenkov, A.V.; Aulchenko, V.M.; Banzarov, V.S.; Bashtovoy, N.S.; Berkaev, D.E.; Bondar, A.E.; Bragin, A.V.; Eidelman, S.I.; et al. Observation of a fine structure in $e^+e^-$ to hadron production at the nucleon-antinucleon threshold. *Phys. Lett.* **2019**, *B794*, 64–68. [CrossRef]
24. Kuraev, E.; Tomasi-Gustafsson, E.; Dbeyssi, A. A Model for space and time-like proton (neutron) form factors. *Phys. Lett.* **2012**, *B712*, 240–244. [CrossRef]
25. Bijker, R.; Iachello, F. Re-analysis of the nucleon space- and time-like electromagnetic form-factors in a two-component model. *Phys. Rev. C* **2004**, *69*, 068201. [CrossRef]
26. Rekalo, M.P. The reaction $\pi + N \to e^+e^- + \pi$. *Sov. J. Nucl.Phys.* **1965**, *1*, 760–765.
27. Adamuscin, C.; Kuraev, E.; Tomasi-Gustafsson, E.; Maas, F. Testing axial and electromagnetic nucleon form factors in time-like regions in the processes $\bar{p} + n \to \pi^- + \ell^+\ell^-$ and $\bar{p} + p \to \pi^0 + \ell^+\ell^-$, $\ell = e, \mu$. *Phys. Rev. C* **2007**, *75*, 045205. [CrossRef]
28. Barucca, G.; Davì, F.; Lancioni, G.; Mengucci, P.; Montalto, L.; Natali, P.P.; Paone, N.; Rinaldi, D.; Scalise, L.; Krusche, B.; et al. PANDA Phase One. *Eur. Phys. J. A* **2021**, *57*, 184. [CrossRef]